

Corrosion Behavior of Pure Copper in Simulated Acid Rain Solutions at Different pH Values: Postprint

Authors: Zhong Wanli, Nie Ming, Liang Yongchun, Ma Yuantai, Li Ying

Date: 2023-03-18T00:00:00+00:00

Abstract

Using electrochemical impedance spectroscopy (EIS), X-ray photoelectron spectroscopy (XPS), and scanning electron microscopy (SEM), the corrosion behavior of pure copper in simulated acid rain solutions with different pH values was investigated. The results indicate that the impedance spectroscopy characteristics of pure copper exhibit significant differences in simulated acid rain solutions with varying pH values, suggesting distinct corrosion mechanisms. XPS analysis shows that at pH 3 of the simulated acid rain solution, Cu₂O is the predominant product formed on the pure copper surface; at pH 5, CuO is the main product; and at pH 6, a mixture of Cu₂O and CuO forms on the surface. Both O₂ and H⁺ influence the corrosion process of pure copper. In low-pH environments, the rate-controlling step of corrosion is the diffusion of dissolved oxygen through the electric double layer, with H⁺ acting as a promoter. As pH increases, the promotional effect of H⁺ gradually weakens, and the corrosion of pure copper becomes primarily controlled by the oxygen depolarization process.

Full Text

Abstract

The corrosion behavior of pure copper in simulated acid rain of different pH was investigated using electrochemical impedance spectroscopy (EIS), X-ray photoelectron spectroscopy (XPS), and scanning electron microscopy (SEM). The results show that the impedance spectra characteristics of pure copper in simulated acid rain solutions with different pH values differ significantly, indicating different corrosion mechanisms. XPS analysis reveals that Cu₂O predominantly forms on the copper surface at pH 3, CuO dominates at pH 5, and a mixture of Cu₂O and CuO forms at pH 6. Both O₂ and H⁺ jointly influence the corrosion process of pure copper. In low pH environments, the rate-controlling step is the

diffusion of dissolved oxygen through the double electric layer, with H^+ promoting the reaction. As pH increases, the promoting effect of H^+ gradually weakens, and copper corrosion becomes primarily controlled by the oxygen depolarization process.

Keywords: metallic materials, materials failure and protection, pure copper, acid rain, corrosion, diffusion

Introduction

Pure copper exhibits excellent electrical and thermal conductivity, leading to widespread application in the power industry. During service, copper corrosion represents the primary constraint on safe equipment operation. Increasingly severe atmospheric pollution in recent years has resulted in frequent acid rain events, drawing greater attention to copper corrosion in acid rain environments. Guangzhou experiences approximately 1700 mm of annual rainfall, and acid rain caused by extensive acidic gas emissions has become a major factor affecting metallic material corrosion in its power systems. Field investigations reveal that acid rain action leads to corrosion product formation on various copper components, causing deterioration of copper's conductive and thermal properties and compromising power system safety. Therefore, in-depth study of copper corrosion mechanisms in acid rain environments and identification of key factors influencing the corrosion process are essential for ensuring safe operation of copper components.

Previous research indicates that copper corrosion mechanisms and products vary with solution pH. In low pH sulfuric acid solutions, copper electrochemical dissolution proceeds through a two-electron autocatalytic process forming Cu^{2+} , while Cu^+ becomes more readily formed at the anode as pH increases [1]. In neutral aqueous solutions, copper anodic dissolution is controlled by Cu^{2+} diffusion within the film [2]. Since copper's standard electrode potential is higher than the hydrogen evolution potential, the cathodic reaction during copper corrosion in acidic solutions is primarily oxygen depolarization [3]. However, the specific influence of high H^+ concentrations in acidic solutions and whether competitive relationships exist with O_2 diffusion require further investigation. This study examines copper corrosion processes in solutions of varying pH to explore the synergistic effects of O_2 and H^+ on copper corrosion mechanisms.

1.1 Sample Preparation and Immersion Testing

T2 pure copper (purity >99.95%) was cut into 15 mm × 15 mm × 2 mm specimens, sequentially ground with SiC abrasive paper, polished with 1 μm diamond paste, rinsed with deionized water and ethanol, and dried with compressed air. To simulate Guangzhou's sulfate-type acid rain, the SO_4^{2-} concentration was increased tenfold, with the specific composition as follows [4]: 42.6 mg/L SO_4^{2-} , 5.2 mg/L Cl^- , 4.25 mg/L NO_3^- , 0.24 mg/L Na^+ , 0.18 mg/L Mg^{2+} , 0.32 mg/L Ca^{2+} , and 1.23 mg/L NH_4^+ . The pH was adjusted with sulfuric acid to pre-

pare three simulated acid rain solutions with pH values of 3, 5, and 6 using analytically pure reagents.

Prepared copper samples were immersed in the simulated acid rain solutions of different pH values at 25°C controlled by a water bath for durations of 1, 5, 25, 50, and 75 h. Electrochemical impedance spectra were measured for each sample during the immersion period, and the surfaces were analyzed using SEM and XPS.

1.2 Electrochemical Impedance Spectroscopy (EIS) Testing

EIS measurements were performed using a PAR 2273 electrochemical workstation (Princeton Applied Research) at open circuit potential. A conventional three-electrode system was employed with a platinum sheet as the auxiliary electrode and a saturated calomel electrode (SCE) as the reference electrode. Samples were connected to copper wire, sealed externally with paraffin and rosin to create working electrodes with an exposed area of 1.5 cm². The frequency range was scanned from 100 kHz to 10 mHz with a 5 mV sinusoidal perturbation signal. Since the self-corrosion potential of the working electrode was unstable at the beginning of measurement, all electrochemical tests commenced only when the self-corrosion potential variation was less than 5 mV within 300 s.

1.3 Characterization of Corrosion Products

The microstructure of copper surfaces after different immersion periods was observed using SEM. Corrosion products were analyzed using an ESCALAB250 XPS system. High-resolution narrow scans were measured with a step size of 0.05 eV, and full spectra were recorded at a photoelectron take-off angle of 51°. In-situ argon ion sputtering was performed under ultra-high vacuum with an ion beam energy of 2 keV, current of approximately 2 mA, and analysis area of a 0.5 mm diameter spot.

2.1 Evolution of Electrochemical Impedance Spectra

[Figure 1: see original paper]-[Figure 3: see original paper] present the impedance spectra of pure copper immersed in simulated acid rain solutions of different pH values for various durations. The impedance spectra show significant differences depending on pH, indicating distinct corrosion mechanisms. At pH 3, the Nyquist plot initially shows a capacitive arc at high frequency and diffusion impedance at low frequency. After 25 h of immersion, an additional capacitive arc appears at medium frequency while diffusion impedance persists at low frequency. This evolution is more clearly observed in the Bode plot, which shows a single peak initially (indicating one time constant corresponding to one capacitive arc) and two peaks after 25 h (indicating two time constants corresponding to two capacitive arcs). These characteristic

changes demonstrate that copper surfaces undergo different corrosion processes throughout the immersion period.

At pH 5, the Nyquist plots after 1 h and 5 h resemble those at pH 3, showing a high-frequency capacitive arc and low-frequency diffusion impedance. However, after 25 h, the low-frequency diffusion impedance disappears and is replaced by another capacitive arc. Comparison of Bode plots for the two pH conditions reveals that although both show two peaks after 25 h, the peak positions in the low-frequency region differ, indicating that the corrosion process at pH 5 differs substantially from that at pH 3. As shown in [Figure 3: see original paper], at pH 6 the impedance spectra characteristics throughout the entire immersion period resemble those at pH 5 after prolonged immersion, with Nyquist plots displaying two capacitive arcs, suggesting similar corrosion mechanisms in these two acidic solutions.

Equivalent circuit analysis is crucial for understanding copper corrosion mechanisms. Based on the differences in impedance spectra across pH values, the equivalent circuit models shown in [Figure 4: see original paper] were used to fit the data. [Figure 4: see original paper]a was used for spectra at pH 3 and pH 5 during 1 h and 5 h immersion, [Figure 4: see original paper]b for pH 3 after 25 h, and [Figure 4: see original paper]c for pH 5 after 25 h and for pH 6. In these circuits, R_s represents solution resistance, R_{ct} charge transfer resistance, R_f film resistance, and W impedance due to diffusion. During actual corrosion processes, constant phase elements (Q) can represent non-ideal capacitance due to surface dispersion effects, where Q_c is the double-layer capacitance and Q_f is the film capacitance. The impedance spectra were fitted using ZsimpWin software based on these equivalent circuits, with results presented in -.

At pH 3, the double-layer capacitance Q_c gradually increases with immersion time, indicating formation of loose corrosion products on the copper surface. Simultaneously, the charge transfer resistance R_{ct} gradually decreases, with a sudden drop at 25 h—coinciding with the appearance of the second capacitive arc in the Nyquist plot. This indicates formation of a corrosion product film with capacitance between 4000 and 6000 $F \cdot cm^{-2}$, suggesting a porous structure. Although film resistance increases with immersion time, its porous structure is insufficient to block transport of aggressive species. These results demonstrate that copper corrosion rate gradually increases with immersion time, and corrosion product formation promotes further corrosion.

At pH 5, the double-layer capacitance shows the same trend as at pH 3 but is one order of magnitude lower, indicating formation of a more compact corrosion product film. The charge transfer resistance follows a similar trend to pH 3, decreasing at 25 h, indicating that the product film also promotes corrosion. However, comparison of film capacitance and resistance after 25 h reveals that both parameters are one order of magnitude smaller than at pH 3, and film resistance increases with time. This suggests that the product film becomes increasingly dense, hindering transport of aggressive species and inhibiting copper corrosion to some extent.

At pH 6, the double-layer capacitance Q_c and charge transfer resistance R_{ct} show opposite trends to those at pH 3: Q_c gradually decreases with immersion time and is two orders of magnitude lower than at pH 3, indicating formation of a more compact product film, while R_{ct} gradually increases, demonstrating that the product film inhibits copper corrosion. Film capacitance and resistance fitting results confirm this conclusion.

Fitting results of EIS in pH=3 solutions

Fitting results of EIS in pH=5 solutions

Fitting results of EIS in pH=6 solutions

2.2 XPS Analysis

[Figure 5: see original paper] shows the Cu2p spectra of corrosion products on copper surfaces. After 25 h immersion at pH 5, the Cu2p_{3/2} binding energy is located at 933.5 eV and Cu2p_{1/2} at 953.3 eV, confirming that the corrosion product is exclusively CuO. The spectrum at pH 6 after 25 h differs significantly, showing distinct shake-up satellite peaks near 940 eV and a shoulder peak near 935.2 eV, indicating that the product contains CuO [5] and possibly other species. Similar features appear after 75 h immersion, with the shake-up peak intensifying at pH 6, confirming CuO presence. Compared to pH 6, the shoulder and shake-up peaks are more intense at pH 5, with Cu2p_{1/2} binding energy near 953.8 eV, indicating CuO as the sole product.

Further analysis of spectra at pH 3 and pH 6 reveals that after 25 h and 75 h immersion, Cu2p_{3/2} binding energy is around 932.8 eV and Cu2p_{1/2} around 952.4 eV. Since both Cu⁺ and Cu⁰ exhibit Cu2p_{3/2} binding energies near 932.6 eV, distinguishing Cu₂O from metallic copper by binding energy alone is difficult. However, Cu₂O and Cu can be differentiated using CuLMM spectra, with kinetic energies of 916.3 eV and 918.3 eV, respectively.

[Figure 6: see original paper] presents the CuLMM spectra. At pH 3, the CuLMM kinetic energy is 916.4 eV (corresponding to Cu₂O) and 918.4 eV (corresponding to metallic copper), with the latter signal arising from the substrate due to the porous Cu₂O structure. At pH 6, kinetic energies are 916.8 eV (Cu₂O) and 917.6 eV (CuO) [4]. Comprehensive analysis confirms that only Cu₂O forms at pH 3, only CuO forms at pH 5, and a mixture of Cu₂O and CuO forms at pH 6.

2.3 Microstructure of Corrosion Products

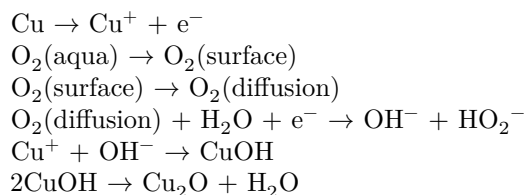
[Figure 7: see original paper] shows the surface microstructure of copper immersed in pH 3 simulated acid rain for various durations. After 25 h, discontinuous amorphous corrosion products form on the surface, identified by XPS as Cu₂O, indicating that high H⁺ concentration in the initial stage inhibits Cu₂O crystal growth. With extended immersion, cubic Cu₂O grains gradually form, though only small amounts appear after 75 h, suggesting dissolution of corrosion

products in high H^+ concentration solutions.

[Figure 8: see original paper] and [Figure 9: see original paper] illustrate microstructural evolution at pH 5 and pH 6. In the initial stage, polishing marks remain visible, indicating a very thin corrosion product film and reduced corrosion rate in low H^+ concentration solutions—consistent with EIS fitting results. At pH 5, flocculent products appear after 50 h, gradually transforming into granular corrosion products with time, indicating formation of intermediate products during corrosion. At pH 6, a uniform dense product film forms with fine particles that increase with time, confirming formation of two corrosion product types and consistent with XPS analysis. The composition and microstructure of copper surfaces change significantly across different pH values, with distinct impedance spectra characteristics indicating different corrosion mechanisms.

2.4 Synergistic Mechanism of O_2 and H^+

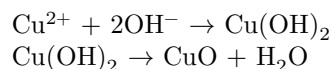
The anodic reaction of pure copper varies significantly with H^+ concentration in acidic solutions. When H^+ concentration exceeds 0.01 mol/L (pH < 2), Cu^{2+} formation is favored at the anode, while Cu^+ formation becomes favorable as H^+ concentration decreases (pH increases) [1]. The type of corrosion product formed and the corrosion mechanism depend on the cathodic reaction [6,7]. At pH 3, diffusion impedance persists throughout the EIS measurements, with corrosion product response signals appearing after 25 h. EIS fitting results indicate the corrosion product is porous and loose. XPS analysis confirms the product is exclusively Cu_2O , meaning O_2 can easily penetrate the corrosion product to reach the copper surface. Thus, O_2 diffusion through the double electric layer controls the corrosion process. The proposed corrosion mechanism at pH 3 is:



Equation (1) represents the rate-controlling step. Due to high H^+ concentration, reaction (2) consumes OH^- , promoting continuous progress of reaction (1). Adsorbed oxygen is rapidly consumed to form OH^- , ultimately generating Cu_2O through the overall reaction.

At pH 5, XPS analysis shows the corrosion product consists solely of CuO , implying the anodic reaction provides Cu^{2+} . However, literature [1] indicates that only Cu^+ forms at the anode under high pH conditions, making dissolved oxygen critical for oxidation. The proposed corrosion mechanism at pH 5 involves initial Cu^+ formation at the copper surface, with simultaneous O_2 diffusion to the solution-copper interface and adsorption, oxidizing Cu^+ to Cu^{2+} through:





The corrosion mechanism at pH 6 is similar to pH 5, with the only difference being formation of a denser product film that hinders O_2 transport. This inhibits reaction (4), preventing complete oxidation of Cu^+ to Cu^{2+} and resulting in a mixed Cu_2O and CuO product.

3 Conclusions

The corrosion products and mechanisms of pure copper in simulated acid rain vary with solution pH. At pH 3, only loose Cu_2O forms on the surface, with corrosion controlled by dissolved oxygen diffusion through the double electric layer and accelerated by H^+ presence. At pH 5, dissolved oxygen oxidizes Cu^+ to Cu^{2+} , forming relatively dense CuO corrosion products with corrosion controlled by oxygen depolarization. At pH 6, the corrosion process is similar to pH 5, but the denser surface film impedes O_2 transport, resulting in incomplete oxidation of Cu^+ and formation of mixed Cu_2O and CuO products.

References

1. Wong D K Y, Coller B A W, MacFarlane D R. A kinetic model for the dissolution mechanism of copper in acid sulfate solutions, *Electrochemical Acta*, 38, 2121(1993)
2. Y. Feng, W. K. Teo, K. S. Siow, G. L. Tan, A. K. Hsieh, The corrosion behavior of copper in neutral tap water. Part I: Corrosion mechanism, *Corrosion Science*, 38, 369(1996)
3. Y. Feng, K. S. Siow, W. K. Teo, G. L. Tan, A. K. Hsieh, Corrosion mechanisms and products of copper in aqueous solutions at various pH values, *Corrosion*, 53, 389(1997)
4. Xu Guo, Wu Yan, Present situation and major ions in acid rain in Guangzhou, *Guangdong Chemical Industry*, 32, 190(2010)
5. Li Xiaoli, Xie Fangyan, Gong Li, Zhang Weihong, Yu Xiaolong, Chen Jian, Effect of argon ion bombardment on copper oxide studied by x-ray photoelectron spectroscopy, *Journal of Instrument Analysis*, 32, 535(2013)
6. An B G, Zhang X Y, Han E H, Corrosion behavior of pure copper during initial exposure stage in atmosphere of Shenyang city, *Acta Metall. Sin.*, 43, 77(2007)
7. Zhang X Y, An B G, Han E H, Corrosion behavior of copper in simulated rain water, *Corrosion Science and Protection Technology*, 14, 257(2002)

Note: Figure translations are in progress. See original paper for figures.

Source: ChinaXiv – Machine translation. Verify with original.